Unidirectional transmission in non-symmetric gratings containing metallic layers

A.E. Serebryannikov[1,*] and Ekmel Ozbay[1]

[1]*Nanotechnology Research Center-NANOTAM, Department of Physics, Department of Electrical and Electronics Engineering, Bilkent University, 06800 Ankara, Turkey*

[*]*andriy@bilkent.edu.tr*

Abstract: The mechanism of achieving unidirectional transmission in the gratings, which only contain isotropic dielectric and metallic layers, is suggested and numerically validated. It is shown that significant transmission in one direction and nearly zero transmission in the opposite direction can be obtained in the same intrinsically isotropic gratings as those studied recently in A. E. Serebryannikov and E. Ozbay, Opt. Express **17**, 278 (2009), but at a non-zero angle of incidence. The tilting, non-symmetric features of the grating and the presence of a metallic layer with a small positive real part of the index of refraction are the conditions that are necessary for obtaining the unidirectionality. Single- and multibeam operational regimes are demonstrated. The frequency and angle ranges of the unidirectional transmission can be estimated by using the conventional framework based on isofrequency dispersion contours and construction lines that properly take into account the periodic features of the interfaces, but should then be corrected because of the tunneling arising within the adjacent ranges. After proper optimization, this mechanism is expected to become an alternative to that based on the use of anisotropic materials.

OCIS codes: (050.1970) Diffractive optics; (050.1960) Diffraction theory; (120.7000) Transmission; (160.4670) Optical materials; (160.3900) Metals.

References and links

1. Z. Wang, J. D. Chong, J. D. Joannopoulos, and M. Soljacic, "Reflection-free one-way edge modes in gyromagnetic photonic crystals," Phys. Rev. Lett. **100**, 013905 (2008).
2. F. D. M. Haldane and S. Raghu, "Possible realization of directional optical waveguides in photonic crystals with broken time-reversal symmetry," arXiv:cond-mat/0503588 (2008).
3. A. Figotin and I. Vitebskiy, "Electromagnetic unidirectionality and frozen modes in magnetic photonic crystals," J. Magnetism Magnet. Mat. **300**, 117 (2006).
4. A. Figotin and I. Vitebskiy, "Electromagnetic unidirectionality in magnetic photonic crystals," Phys. Rev. B **67**, 165210 (2003).
5. C. Luo, S. G. Johnson, J. D. Joannopoulos, and J. B. Pendry, "All-angle negative refraction without negative effective index," Phys. Rev. B **65**, 201104 (2002).
6. A. E. Serebryannikov, T. Magath, and K. Schuenemann, "Bragg transmittance of *s*-polarized waves through finite-thickness photonic crystals with a periodically corrugated interface," Phys. Rev. E **74**, 066607 (2006).
7. M. J. Lockyear, A. P. Hibbins, K. R. White, and J. R. Sambles, "One-way diffraction grating," Phys. Rev. E **74**, 056611 (2006).
8. A.E. Serebryannikov, T. Magath, K. Schuenemann, and O.Y. Vasylchenko, "Scattering of *s*-polarized plane waves by finite-thickness periodic structures made of ultralow-permittivity metamaterials," Phys. Rev. B **73**, 115111 (2006).
9. A.E. Serebryannikov and E. Ozbay, "Isolation and one-way effects in diffraction on dielectric gratings with plasmonic inserts," Opt. Express **17**, 278 (2009).
10. A. Alu, M. G. Silveirinha, A. Salandrino, and N. Engheta, "Epsilon-near-zero metamaterials and electromagnetic sources: Tailoring the radiation phase pattern," Phys. Rev. B **75**, 155410 (2007).
11. R. W. Ziolkowski, "Propagation in and scattering from a matched metamaterial having a zero index of refraction," Phys. Rev. E **70**, 046608 (2004).
12. J. M. Steele, C. E. Moran, A. Lee, C. M. Aguirre, and N. J. Halas, "Metallodielectric gratings with subwavelength slots: Optical properties, " Phys. Rev. B **68**, 205103 (2003).

#111241 - $15.00 USD Received 11 May 2009; revised 9 Jul 2009; accepted 13 Jul 2009; published 20 Jul 2009

13. K. G. Lee and Q-H. Park, "Coupling of surface plasmon polaritons and light in metallic nanoslits," Phys. Rev. Lett. **95**, 103902 (2005).
14. A. Barbara, P, Quemerais, E. Bustarret, and T. Lopez-Rios, "Optical transmission through subwavelength metallic gratings," Phys. Rev. B **66**, 161403 (2002).
15. D. Felbacq, M.C. Larciprete, C. Sibilia, M. Bertolotti, and M. Scalora, "Multiple wavelength filtering of light through inner resonances," Phys. Rev. E **72**, 066610 (2005).
16. A. Sihvola, *Electromagnetic mixing formulas and applications* (IEE, London, 1999).
17. J. B. Pendry, A. J. Holden, W. J. Stewart, and I. Youngs, "Extremely low frequency plasmons in metallic mesostructures," Phys. Rev. Lett. **76**, 4773-4776 (1996).
18. B. T. Schwartz and R. Piestun, "Total external reflection from metamaterials with ultralow refractive index," J. Opt. Soc. Am. B **20**, 2448-2453 (2003).
19. S. Enoch, G. Tayeb, P. Sabouroux, N. Guerin, and P. Vincent, "A metamaterial for directive emission," Phys. Rev. Lett. **89**, 213902 (2002).
20. M. Silverinha and N. Engheta, "Design of matched zero-index metamaterials using non-magnetic inclusions in epsilon-near-zero media," Phys. Rev. B **75**, 075119 (2007).
21. T. Magath and A. E. Serebryannikov, "Fast iterative, coupled-integral-equation technique for inhomogeneous profiled and periodic slabs," J. Opt. Soc. Am. A **22**, 2405-2418 (2005).

1. Introduction

In recent studies it has been shown that reflection-free unidirectional transmission can be realized due to the one-way edge modes arising in two-dimensional gyromagnetic photonic crystals, which are stacked with two-dimensional isotropic photonic crystals [1]. This mechanism has been initially suggested for stacks of two magneto-optic photonic crystals, by using the analogy with the chiral edge states in the quantum Hall effect [2]. The possibility of unidirectional transmission has been demonstrated recently in magnetic photonic crystals, which represent one-dimensional periodic arrays of alternating layers made of lossless materials, at least one of which is magnetically polarized [3,4].

Some features of anisotropic media can be mimicked by photonic crystals that are made of purely isotropic constituents. For example, anisotropy-like dispersion can be obtained, i.e. the isofrequency dispersion contours are localized at a periphery point of the First Brillouin Zone [5]. In this case, one-way higher-order transmission and even unidirectional transmission can be obtained, provided that the front-side and back-side interfaces have different periods [6]. One-way transmission might also appear in metallic slabs with the branched multiple slits [7] and gratings made of a zero-permittivity material [8], so that an anisotropy-like dispersion is not needed. While zero-order transmission is reciprocal, being independent of whether the corrugated or non-corrugated interface is illuminated, higher-order transmission can depend on the direction of the illumination, being associated with one-way transmission. This regime can be considered as *partial unidirectionality*. The different periods of the two interfaces, i.e. no symmetry with respect to the middle plane, is a common feature of the mentioned three classes of the periodic structures.

Recently, non-symmetric gratings containing the corrugated and flat dielectric layers as well as a flat metallic layer have been suggested for obtaining a wideband one-way transmission at normal incidence [9]. This regime is realizable since the number of propagating orders in a lossless ultralow-positive-index medium can be smaller than in the air and dielectric material of the layers. The observed order selectivity can be interpreted in terms of *isolation*, because the far field in the transmission half-space does not contain any order that could be created owing to the corrugation of the front-side (illumination) interface, or it contains only a part of these orders. This effect is similar to the isolation that was studied recently for the slabs made of epsilon-near-zero [10] and matched-impedance zero-index artificial materials [11]. According to [9], neither the permittivity nor the index is necessarily (near-)zero for obtaining isolation. In fact, their values may be within a rather wide range of variation. At the same time, the near-field features associated with isolation and one-way transmission either have been observed or are expected to be observed in the gratings of another type, which still contain metallic constituents [12]-[15].

In the present paper, we will theoretically show that at least *imperfect unidirectionality* can be obtained for the gratings with layers showing *isotropic* dispersion, so that significant

#111241 - $15.00 USD Received 11 May 2009; revised 9 Jul 2009; accepted 13 Jul 2009; published 20 Jul 2009

transmission occurs if the grating is illuminated from the side of the corrugated interface but vanishes if it is illuminated from the side of the flat interface. Hence, an anisotropy-like transmission can be obtained even without anisotropy-like dispersion. This can be achieved due to tilting, which makes the zero order in air and dielectric layer(s) uncoupled to that in the collisionless metallic layer, while at least one higher order is coupled. Furthermore, the dominance of certain orders in transmission can be realized by varying the angle of incidence and choosing proper parameters of the corrugations and metallic layer. In particular, single-beam and multibeam unidirectionality with the equal contribution of higher orders, or dominant contribution of one of them will be demonstrated.

Most of the presented results are obtained for either the same or similar parameters as those used in [9] at normal incidence. The main goal of the present paper is the demonstration of the principal possibility of achieving unidirectionality rather than a design-related study. It is noteworthy that in the suggested approach the unidirectional transmission only involves linearly polarized waves. This is distinguished from the approaches based on the use of anisotropic materials, which involve the elliptically and circularly polarized waves. It is assumed that the permittivity of the metallic layer depends on frequency, according to the Drude model. Therefore, the observed effects can be assigned to a wide frequency range, so that the suggested approach can also be realized using the composed media, whose permittivity corresponds to the Drude model [16,17]. In line with [17], Drude-type dispersion can be scaled down to microwave frequencies in the arrays of thin metallic rods. An example of rod arrays that are associated with metamaterials, which have an ultralow positive index at optical frequencies can be found in [18]. Several performances of epsilon-near-zero and matched-impedance zero-index metamaterials have been suggested in [11,19,20]. The presented transmission and reflection results are obtained by using an original computer code, which is based on the fast coupled-integral-equations technique [21].

2. Theoretical background

The general geometry of the studied gratings is shown in the left plot in Fig. 1. They consist of a flat metallic layer as well as corrugated and flat dielectric layers. The upper and lower interfaces are assumed to be set by

$$f_1(x) = A + B\cos(2\pi xM / L) \qquad \text{and} \qquad f_2(x) = C + D\cos(2\pi xM / L)\,. \tag{1}$$

The structure shown in the left plot in Fig. 1 is similar to the ones that are referred to as U structures, if the Upper (front-side) interface is corrugated. Correspondingly, a structure with the corrugated Lower (back-side) interface is referred to as an L structure. If B=0 and $D \neq 0$, we obtain an L structure. In turn, U structures correspond to $B \neq 0$ and D=0. ε_U and ε_L stand for the permittivity of the upper and lower dielectric layers, respectively. The permittivity of the metallic layer (a<y<b) varies with the angular frequency ω according to the Drude model:

$$\varepsilon_m(\omega) = 1 - \omega_p^2/[\omega(\omega + i\gamma)]\,,$$

where ω_p and γ mean the plasma and collision frequencies. It is assumed that $A + B \le 1$, $C - D \ge 0$, $C + D \le a$, $A - B \ge b$, so that for the maximal thickness of the grating, h, we have h=A+B-(C-D). Consideration is restricted to the case of s-polarization. The incident wave is given by $E_z^i(x,y) = E_0\exp(i\alpha_0 x - i\beta_0 y)$, where $\alpha_0 = k\sin\theta$, $\beta_0 = k\cos\theta$, k=ω/c, and θ is the angle of incidence. The diffraction efficiencies are given by

$$t_n = \tau_n\tau_n^*\mathrm{Re}\,\beta_n/W \qquad \text{and} \qquad r_n = \rho_n\rho_n^*\mathrm{Re}\,\beta_n/W\,, \tag{2}$$

where W is the energy of the incident wave, τ_n and ρ_n are the nth-order transmission and reflection coefficients, $\beta_n = [k^2 - \alpha_n^2]^{1/2}$, $\alpha_n = \alpha_0 + 2\pi nM/L$, and the asterisk means complex conjugate. W=R+T+A where R, T, and A are reflectance, transmittance, and

#111241 - $15.00 USD Received 11 May 2009; revised 9 Jul 2009; accepted 13 Jul 2009; published 20 Jul 2009

absorptance, respectively. It is expected that the order selectivity can be realized due to the effect of the metallic layer, while the dielectric layers should provide a high index contrast at the interfaces. Hence, the contribution of t_n and r_n to T and R can be enhanced or weakened due to the proper choice of ε_U and ε_L. The nth-order beam propagates in air at $k > |\alpha_0 + 2\pi nM/kL|$. The angles of diffraction ϕ_n depend on θ according to the equation $\sin\phi_n = \sin\theta + 2\pi nM/kL$.

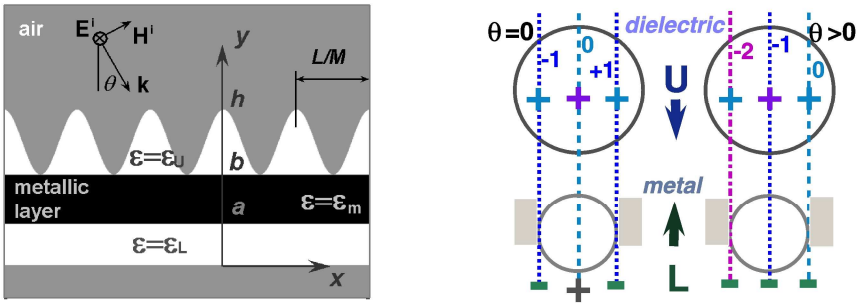

Fig. 1. Left plot: Three-layer grating illuminated by *s*-polarized plane wave at a non-zero θ; Right plot: isofrequency dispersion contours in dielectric and metal and construction lines at the interface between the flat metallic layer and the corrugated dielectric layer at θ=0 and θ>0; arrows – direction of incidence in U and L cases at θ=0.

It can be shown that the nth order propagates in a collisionless Drude medium (γ=0) starting from a larger k than in air, i.e. $k=\kappa_n > |\alpha_0 + 2\pi nM/kL|$, which can be found at M=1 from the following equation:

$$\kappa_n L = \chi^{-2}\left[2\pi n\sin\theta + \sqrt{(2\pi n)^2 + (\chi\omega_p L/c)^2}\right], \tag{3}$$

where $\chi = \cos\theta$. At n=0, $\kappa_0 L = \omega_p L/c\chi$. Correspondingly, the range of the variation of θ, in which the propagating nth order in air or dielectric is coupled to the propagating nth order in a Drude medium at fixed kL, is limited by $\psi_n < \theta < \varphi_n$, where

$$\psi_n = -\pi/2 \qquad \text{and} \qquad \varphi_n = \sin^{-1}(\Theta_n/kL) \tag{4}$$

for n>0, and

$$\psi_n = \sin^{-1}(\Omega_n/kL) \qquad \text{and} \qquad \varphi_n = \pi/2 \tag{5}$$

for n<0, provided that $\Omega_n/kL < -1$ in Eq. (4) and $\Theta_n/kL > 1$ in Eq. (5). In turn, $\Theta_n = -2\pi n + \Lambda_n$ and $\Omega_n = -2\pi n - \Lambda_n$, and $\Lambda_n = \sqrt{(kL)^2 - (\omega_p L/c)^2}$. The features of the ω-domain thresholds, κ_n, and θ-domain boundaries of the nth-order propagation range, ψ_n and φ_n, can be visualized by using the conventional approach based on the isofrequency dispersion contours for the dielectric and metallic media and the construction lines, which take into account the periodic features of the interfaces and the orientation of the corrugated interface with respect to the incident wave.

An example is shown in the right plot in Fig. 1. The left subplot corresponds to $k=\kappa_{\pm 1}$ and θ=0, so that zero order is only coupled to a propagating order in a collisionless metal, regardless of whether the corrugated interface (U case) or non-corrugated interface (L case) is illuminated. As a result, a single transmission channel is open in both cases and transmission is reciprocal, i.e. $t_0^L = t_0^U$. This case corresponds to the *bidirectional isolation* regime, since no

#111241 - $15.00 USD Received 11 May 2009; revised 9 Jul 2009; accepted 13 Jul 2009; published 20 Jul 2009

corrugation feature is transferred through the structure in the U case. In the L case, negative-first-order transmission is expected to occur due to the effect of the corrugated (back-side) interface, leading to the fact that $t_n^{\mathrm{L}} \neq t_n^{\mathrm{U}}$ for the propagating orders with $|n|=1$ and, hence, to one-way transmission like that studied in [9]. Generally speaking, non-reciprocal higher-order transmission is a typical feature even for non-symmetric purely dielectric gratings. However, a proper manipulation by the properties of transmission channels, i.e. open or closed, cannot be obtained without the narrowing of isofrequency contours. This feature is achievable due to the use of a metallic layer. Based on this consideration, we can expect that the unidirectional transmission, i.e. non-zero T^{U} and zero T^{L} can be realized at least if the propagating zero order in the corrugated dielectric layer is uncoupled to the zero order in metal at $\gamma=0$, while at least one of the higher orders remains coupled. The right subplot in Fig. 1(b) demonstrates that this can simply be obtained by tilting. Here, $k=\kappa_{-2}=\kappa_0$ so that the order with $n=-1$ is only coupled in the U case. At the same time, no transmission channel is open in the L case because of the absence of corrugations on the front-side interface.

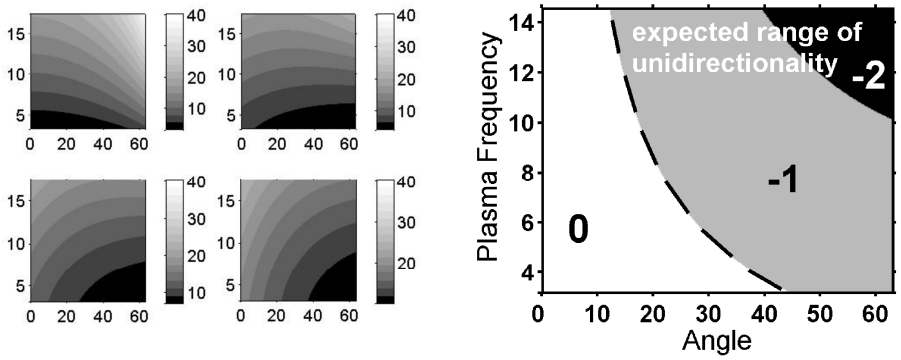

Fig. 2. Values of $\kappa_n L$ on the plane of $(\theta,\omega_p L/c)$ for $n=0$ (upper left), $n=-1$ (upper right), $n=-2$ (lower left), and $n=-3$ (lower right) – left plot; zones corresponding to the different diffraction orders with $\min\kappa_n L$ on the plane of $(\theta,\omega_p L/c)$ – right plot; θ is shown in degrees.

Hence, the necessary condition of unidirectionality is that at least one of the higher orders in metal is propagating, while zero order is still uncoupled. In other words, a higher-order threshold in metal should appear at a smaller ω than the zero-order one, i.e. the condition

$$\kappa_0(\theta,\omega_p) > \kappa_n(\theta,\omega_p) \tag{6}$$

should be satisfied at least for one of the values of $|n|>0$. Calculations of $\kappa_n L$ vs θ and ω_p were performed using Eq. (3). The obtained results are shown in the left plot in Fig. 2. It is seen that κ_0 and κ_n at $|n|>0$ may show the opposite trends of variation with θ. Based on these results, the zones of $\min\kappa_n L$ have been detected, which correspond to different n, see the right plot in Fig. 2. The dashed line corresponds to $\min\kappa_n L=\kappa_0 L$ that is the boundary of the zone where unidirectional transmission might appear. This line is given by the equation

$$\omega_p L/c = \pi\cot\theta, \tag{7}$$

that is equivalent to $\kappa_0=\kappa_{-1}$ where κ_0 and κ_{-1} are replaced by the right-hand side of Eq. (3) for the corresponding values of n. The boundary between the ranges of $\min\kappa_n L=\kappa_{-1}L$ and $\min\kappa_n L=\kappa_{-2}L$ is given by

$$\omega_p L/c = 2\pi\Phi(\theta)/\sin 2\theta, \tag{8}$$

#111241 - $15.00 USD Received 11 May 2009; revised 9 Jul 2009; accepted 13 Jul 2009; published 20 Jul 2009

where $\Phi(\theta) = \sqrt{9\text{-}\sin^2\theta\,(10\text{-}\sin^2\theta)}$.

3. Results and discussion

3.1 Basic effects

Figure 3 shows an example of the effect of changing the side of illumination for a finite-thickness three-layer grating with one-side sinusoidal corrugations. For the convenience of comparison, geometrical parameters were taken just as in one of the cases that was studied in [9]. The only difference is that a non-zero angle of incidence is now being used. One can see that for the considered *kL*-range the unidirectional transmission is strongly pronounced, so that $T^{\mathrm{U}}/T^{\mathrm{L}} \geq 100$ at $kL \geq 13$ and $\max T^{\mathrm{U}}/T^{\mathrm{L}} = 970$ at $kL \approx 16.2$. This feature is in agreement with the interpretation based on the dispersion results. Indeed, when the structure is illuminated from the side of the corrugated dielectric layer (U case), the zero order in the dielectric is not coupled to a propagating order in the collisionless metal, that leads to $t_0^{\mathrm{U}} \approx 0$.

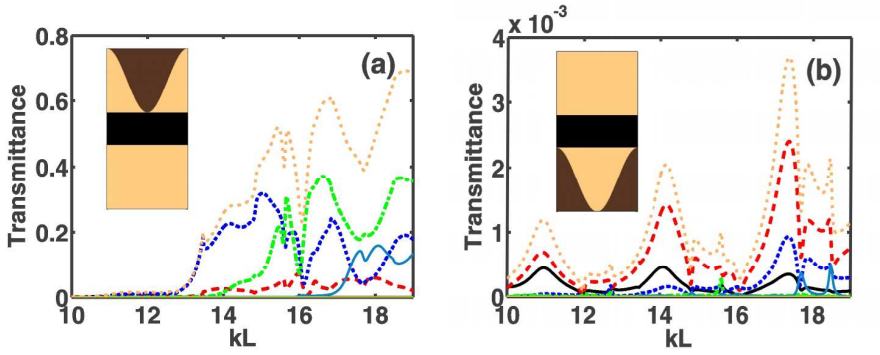

Fig. 3. Transmittance for a three-layer grating in the cases U (a) and L (b); A=0.8, B=0.2, and C=D=0, in U case, and A=1, B=0, and C=D=0.2 in L case; ε_{U}=ε_{L}=2.1, h/L=2, a/h=0.4, b/h=0.6, $\omega_p L/c$=4π, γ/ω_p=0.01, θ=π/3, and M=1; black solid line – n=0, red dashed line - n=–1, blue thick dotted line - n=–2, green dashed-dotted line - n=–3, blue solid line - n=–4, orange thin dotted line – sum of all the propagating orders.

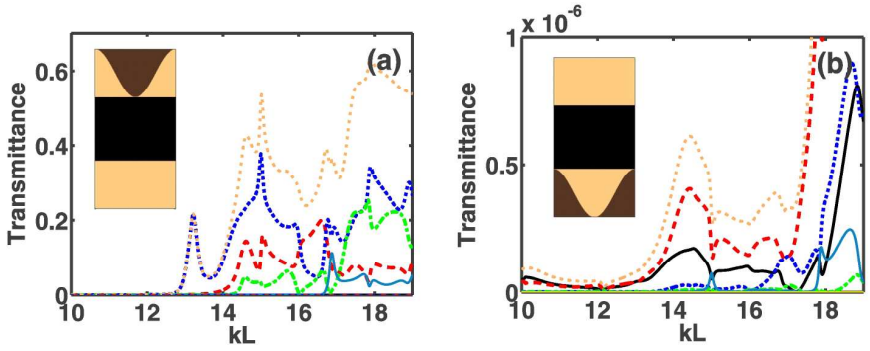

Fig. 4. Same as Fig. 3, except for A=0.85 and B=0.15 in the U case, C=D=0.15 in the L case, and a/h=0.3 and b/h=0.7.

However, higher orders in the dielectric are coupled to those in the metal, in turn leading to rather large T^{U}, as seen in Fig. 3(a). If the same structure is illuminated from the side of the non-corrugated inteface (L case), there is only one order (zero order), which propagates in the dielectric layer, but it is not coupled to that in the metal. This example demonstrates that an anisotropic-like unidirectional transmission can be achieved due to the tilting of the structures,

#111241 - $15.00 USD Received 11 May 2009; revised 9 Jul 2009; accepted 13 Jul 2009; published 20 Jul 2009

which are intrinsically isotropic. The non-zero values of T^{L} can be connected with a weak tunneling.

Let us compare the values of κ_n obtained from Eq. (3), and the values of $k=K_n$ starting from which higher orders actually contribute to T^{U}. For the parameters used in Fig. 3(a), $\kappa_n L$ is equal to 8π, 13.78, 12.67, 14.18, and 16.56 for n=0,–1,–2,–3, and –4, respectively, while $\kappa_0 c/\omega_p$=2. The values of ϕ_n at n=–1,–2,–3, and –4 are equal to 24.2°, –6.8°, –27.6°, and –40.7°. Comparing to Fig. 3(a), one can see that Eq. (3) correctly predicts the order of the actual thresholds at various n with respect to each other. The values of $K_n L$, starting from which $T^{\mathrm{U}}>10^{-3}$, are equal to 10.62, 10.18, 12.73, and 15.88 for n=–1,–2,–3, and –4, respectively. The widening of the range of the actual contribution of the nth order at $k<\kappa_n$ takes place due to the contribution of evanescent waves. However, t_n keep relatively small values here, while the enhancement of their contribution occurs in the vicinity of $k=\kappa_n$.

The basic transmission features that are shown in Fig. 3 remain within a wide range of variation of the problem parameters. Figure 4 shows the appearance of unidirectionality in the grating with a thicker metallic layer and less deep corrugations than in Fig. 3. (It has also been studied at θ=0 in [9]). The increase of $(b-a)/h$ results in the weakening of the tunneling, especially in the L case, so that now $T^{\mathrm{U}}/T^{\mathrm{L}} \geq 10^5$ at $kL \geq 12.74$ and $\max T^{\mathrm{U}}/T^{\mathrm{L}} = 2.1\times10^6$ at $kL \approx 13.2$. The values of $K_n L$ are equal to 13.26, 12.44, 14.15, and 16.59 for n=–1,–2,–3, and –4, respectively. This means that the tunneling is weakened so that $K_n \approx \kappa_n$ at least for n<–2. It is noteworthy that the *single-beam unidirectional regime* in Fig. 4(a) is realized due to the order with n=–2, i.e. at $K_{-2}<k<K_{-1}$, showing the maximum of t_{-2}=0.22 at kL=13.22 and ϕ_{-2}=–4.8°. In the comparison, in Fig. 3(a), t_{-2}=0.18 and t_{-1}=0.01 at kL=13.47 (ϕ_{-2}=–3.8° and ϕ_{-1}=23.6°). The *multibeam unidirectional regime* with $t_{-2}=t_{-3}$=0.22 is observed in Fig. 4(a) at kL=17.6. The largest values of T^{U} are achieved in Fig. 4(a) at kL=17.88 (T^{U}=0.64) and in Fig. 3(a) at kL=18.8 (T^{U}=0.69).

3.2 Gratings with smaller thickness

Now, we demonstrate that strong unidirectionality can occur for the gratings, which are thinner than those in Figs. 3 and 4. Figure 5 shows t_n vs kL in the U case for the grating with the same $(b-a)/L$ but smaller h/L than in Fig. 3. For the L-case counterpart, $t_n^{\mathrm{L}} << t_n^{\mathrm{U}}$ at least within the ranges of the significant contribution of the several first orders to T^{U} in a similar fashion as in Figs. 3 and 4. Therefore, we further consider the U case only.

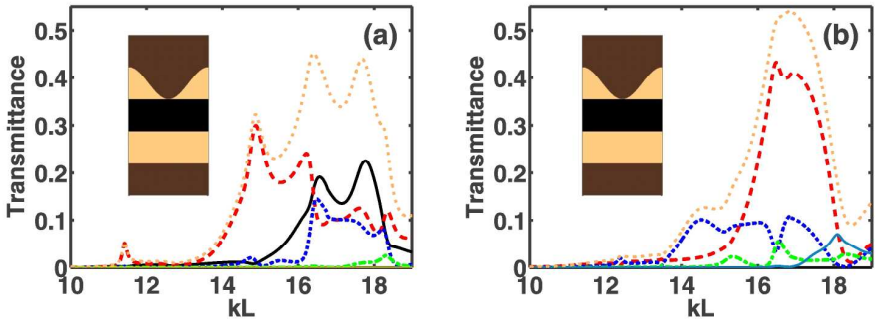

Fig. 5. Same as Fig. 3(a), except for A=0.7, B=0.1, C=0.2, D=0, and h/L=1.2; $\theta=\pi/6$ in plot (a) and $\theta=\pi/3$ in plot (b).

Figure 5(a) shows that the strong difference between T^{U} and T^{L} can also be achieved when $\kappa_0 c/\omega_p$ is smaller than in Figs. 3 and 4. At $\theta=\pi/6$, $\kappa_n L$=14.51, 4π, 13.79, 16.45, and 19.76 for n=0,–1,–2,–3, and –4, respectively, and $\kappa_0 c/\omega_p$=1.155. Hence, it is expected that the order

#111241 - $15.00 USD Received 11 May 2009; revised 9 Jul 2009; accepted 13 Jul 2009; published 20 Jul 2009

with n=−1 prevails in the propagating-wave originated transmission in the range right above kL= $\omega_p L/c$. All the orders contribute to T^{U} starting from k=K_n< κ_n due to tunneling. t_{-1} remains the basic contributor at least at kL<15, while $\max t_{-1} \approx 0.3$ and $T^{\mathrm{U}} \approx 0.32$ at kL=14.87. Furthermore, the negative first order dominates in the evanescent-wave originated transmission, i.e. at kL<$\omega_p L/c$, where t_{-1} reaches 0.05 at kL=11.42. Within the range of large t_0^{U}, the partial unidirectionality leads, in particular, to the *unidirectional splitting* at kL=16.43, where $t_{-1}^{\mathrm{U}} = t_{-2}^{\mathrm{U}} \approx 0.14$ and $T^{\mathrm{L}} = t_0^{\mathrm{L}} = t_0^{\mathrm{U}}$. This regime is similar to those studied at θ=0 in [9].

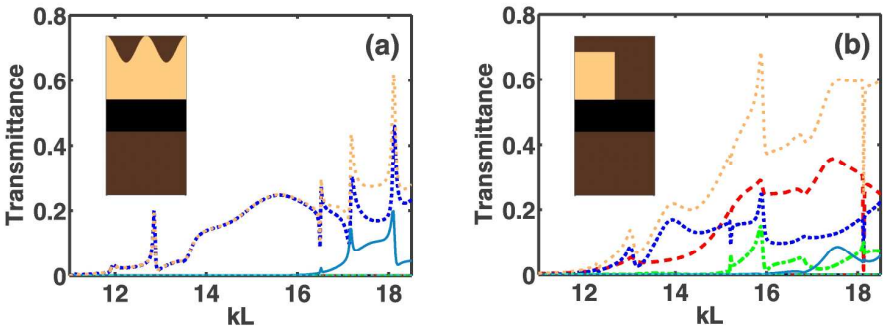

Fig. 6. Transmittance for two-layer gratings in the U case at θ=π/3, a/h=0.4, b/h=0.6, $\omega_p L/c$=4π, and γ/ω_p=0.01; plot (a) - A=1−B, B=0.0833, M=2, ε_{U}=2.1, h/L=1.2; plot (b) – lamellar bars of the height 0.6L, width 0.5L, and permittivity $\varepsilon_{\mathrm{bar}}$=2.1, which are placed on the metallic layer, M=1 and h/L=1; black solid line – n=0 ($t_0 \approx 0$), red dashed line - n=−1, blue thick dotted line - n=−2, green dashed-dotted line - n=−3, blue solid line - n=−4, orange thin dotted line – sum of all the propagating orders.

The kL-range with the dominant contribution of the order with n=−1 also appears at θ=π/3, see Fig. 5(b). In this case, the values of $\kappa_n L$ are the same as in Figs. 3(a) and 4(a). However, in contrast to these figures, t_{-2}<0.101 in Fig. 5(b) within the range of the dominant contribution of the order with n=−2. On the other hand, $\max t_{-1}^{\mathrm{U}} \approx 0.43$ and $T^{\mathrm{U}} \approx 0.52$ at kL=16.48. In fact, this case can be considered as the unidirectional transmission with one main and two parasitic beams.

In Fig. 6, t_n vs kL are presented for the two thin two-layer gratings, showing in the U case the upper corrugated dielectric layer and lower metallic flat layer. In Fig. 6(a), the actual grating period is two times smaller than in the previous figures. However, the order nomenclature is kept the same for the purposes of a comparison, i.e. we assume that $t_{2n+1} \equiv 0$ at $n = 0, \pm 1, \pm 2, \ldots$. The lamellar grating in Fig. 6(b) is topologically similar to but distinguished in material of the flat layer and bars from the gratings considered in the studies of surface-plasmon assisted transmission through the subwavelength slits, that occurs for p-polarization [12]-[14].

Figure 6(a) shows that the range of single-beam unidirectional transmission can be extended by decreasing the actual grating period. Here, it occurs between kL=$K_{-2}L$<11 and kL=$K_{-4}L$=15.81. It is also noteworthy that $K_{-2}L$ is nearly the same here as in Fig. 3(a), but smaller than in Fig. 4(a). Figure 6(b) illustrates the peculiar features of t_n vs kL for the lamellar grating with the same metallic layer as in Figs. 3, 5, and 6(a). Tunneling at k<K_n appears in Fig. 6(b) in such a way that t_{-1} and t_{-2} exceed 0.01 at nearly the same value of $kL \approx 12.1$, so that the range of a significant dominance of the order with n=−2 does not exist. As a result, only the multibeam unidirectionality can be obtained. In Figs. 6(a) and 6(b), $\max T^{\mathrm{U}} > 0.6$, i.e. nearly the same portion of the incident-wave energy is transmitted as for the thick gratings shown in Figs. 3(a) and 4(a).

#111241 - $15.00 USD Received 11 May 2009; revised 9 Jul 2009; accepted 13 Jul 2009; published 20 Jul 2009

3.3 Angle-domain unidirectionality

In this section, we consider the appearance of unidirectionality in θ-domain. In Fig. 7, the transmission results are presented for the same grating parameters as in Fig. 4, except for $\omega_p L/c=2\pi$. A smaller $\omega_p L/c$ is used here in order to avoid the simultaneous contribution of multiple higher orders, which could lead to some difficulties in the interpretation of the results. Figure 7(a) shows t_n vs kL in the U case at $\theta=\pi/3$. One can see that the frequency-domain transmission features observed in Fig. 4(a) remain. The only difference is that now the order with $n=-1$ appears first in the vicinity of $\omega=\omega_p$, leading to the single-beam wideband unidirectionality. This is in agreement with Eq. (3). For the used parameters, $\kappa_n L$ is equal to 4π, 6.33, 8.28, and 11.14 for $n=0,-1,-2$, and -3, respectively, while $\kappa_0 c/\omega_p=2$. In addition to the single-beam wideband unidirectionality, the narrowband effect occurs at $kL=10$ where $t_{-1}=0.38$ and $T=0.395$. A similar narrowband behavior is often observed in the conventional dielectric gratings, but here it manifests itself in a unidirectional fashion due to the stacking of the dielectric and metallic layers.

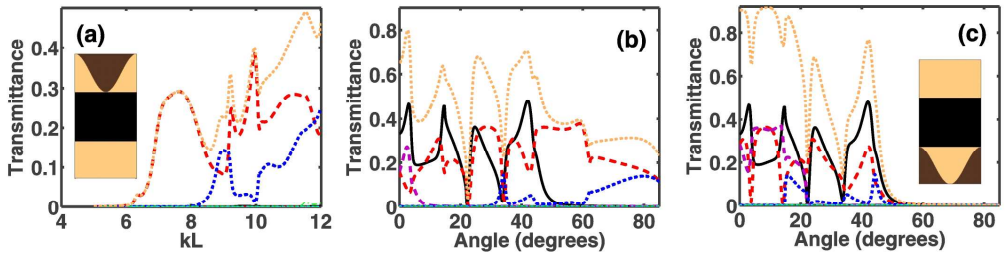

Fig. 7. Transmittance at the same parameters as in Fig. 4, except for $\omega_p L/c=2\pi$: plot (a) – frequency dependence in the U case at $\theta=\pi/3$, plot (b) – angle dependence in the U case at $kL=10$, plot (c) – angle dependence in the L case at $kL=10$; black solid line - $n=0$, red dashed line - $n=-1$, violet dashed line - $n=1$, blue dotted line - $n=-2$, and orange dotted line – sum of all the propagating orders.

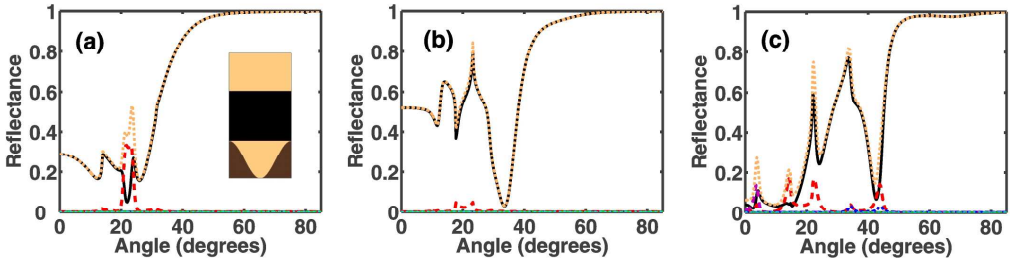

Fig. 8. Angle dependence of reflectance in the L case at the same parameters as in Fig. 4, except for $\omega_p L/c=2\pi$: plot (a) - $kL=8.25$, plot (b) - $kL=9$, and plot (c) - $kL=10$; black solid line - $n=0$, red dashed line - $n=-1$, violet dashed line - $n=1$, and blue dotted line - $n=-2$.

For this specific kL-value, t_n vs θ are shown for the U case in Fig. 7(b) and for the L case in Fig. 7(c). It is seen from the comparison of Fig. 7(b) with Fig. 7(c) that the range of $50°<\theta<80°$ can be considered as that of the two-beam imperfect unidirectionality, since $t_0^{\mathrm{U}}=t_0^{\mathrm{L}}<0.02$ and $t_{-1}^{\mathrm{U}}>0.16$. At $\theta>68°$, $t_0^{\mathrm{U}}=t_0^{\mathrm{L}}<10^{-3}$. The ranges of the significant contribution of the orders with $n=0$, +1 and −2 to T^{U} are in good agreement with Eq. (5). In particular, $\varphi_0^{\mathrm{U}}=51.1°$, $\varphi_{+1}^{\mathrm{U}}=8.6°$ and $\psi_{-2}^{\mathrm{U}}=28.6°$. The ranges of the actual contribution are a bit wider due to the tunneling. In turn, the values of $\varphi_{+1}^{\mathrm{L}}=21.8°$ and $\psi_{-2}^{\mathrm{L}}=14.9°$ obtained for the back-side air half-space correspond well to the boundaries of the range of the actual

#111241 - $15.00 USD Received 11 May 2009; revised 9 Jul 2009; accepted 13 Jul 2009; published 20 Jul 2009

contribution of the orders with n=+1 and n=–2 to T^{L}, demonstrating the role of back-side corrugations in the appearance of non-zero t_n at $|n|>0$, while the higher-order transmission channels in metal are closed. The differences in the values of φ_n and ψ_n in the U and L cases result in the appearance of wide θ-ranges, where higher orders show one-way transmission. The anomalous narrowband transmission effect occurs at θ=22.25°, where t_0<0.01, T^{L} >0.2 and T^{U} <0.04, so that the transmission is suppressed while illuminating the grating from the side of the corrugated interface, leading to *inverse* unidirectionality.

It has been shown in [9] that isolation appears in the reflection mode in ω-domain, which manifests itself in that the back-side corrugations in the L case do not lead to the appearance of the diffracted beams ($|n|>0$) in the half-space above the front-side interface. Figure 8 demonstrates the similar effect arising in θ-domain. According to Eq. (5), $\psi^{\mathrm{L}}_{-1}=6.52°$ and $\psi^{\mathrm{L}}_{-2}=61.1°$ in Fig. 8(a), $\psi^{\mathrm{L}}_{-1}=-1.02°$ and $\psi^{\mathrm{L}}_{-2}=42.9°$ in Fig. 8(b), and $\psi^{\mathrm{L}}_{-1}=-8.6°$ and $\psi^{\mathrm{L}}_{-2}=28.6°$ in Fig. 8(c), $\psi^{\mathrm{L}}_{n}=-\varphi^{\mathrm{L}}_{-n}$. One can see that the ranges of the actual contribution of higher orders to R^{L} are much narrower. They do not contribute within any of the zero-order forbidden θ-ranges, i.e. at θ>40.4° in Fig. 8(a), θ >45.7° in Fig. 8(b), and θ >51.1° in Fig. 8(c), and within smaller-θ ranges where the zero order is propagating in metal in line with Eq. (5), and hence at least one channel is open. The difference between the propagating-wave ranges with the vanishing and substantial role of the corrugations cannot be detected from the dispersion results. Despite the narrowing ranges of higher-order reflection, its contribution to R^{L} can still be significant, e.g. in the vicinity of θ=20° in Fig. 8(a). The above-reported

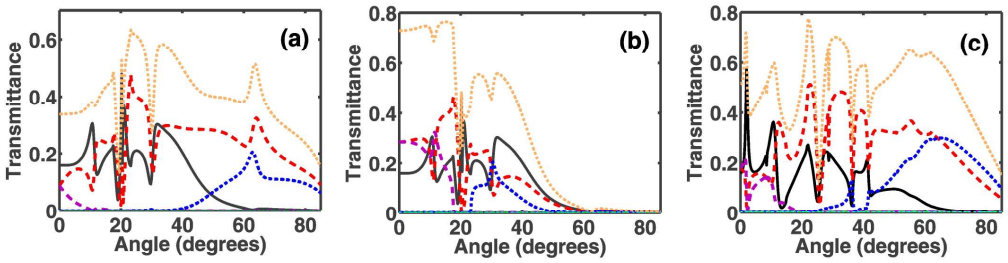

Fig. 9. Angle dependence of transmittance at the same parameters as in Fig. 3 except for $\omega_p L/c=2\pi$: plot (a) – U case, kL=9, plot (b) – L case, kL=9, plot (c) – U case, kL=10; black solid line - n=0, red dashed line - n=–1, violet dashed line - n=1, blue dotted line - n=–2, and orange dotted line – sum of all the propagating orders.

diffraction features remain within a wide range of parameter variation. As an example, Fig. 9 shows t_n vs θ for a grating, which differs from that in Fig. 3 in smaller $\omega_p L/c$. Now, it is the same as in Figs. 7 and 8. The appearance of the multibeam unidirectionality at $\theta>\pi/3$ can be seen from the comparison of Figs. 9(a) and 9(b). Here, maxT^{U}=0.51 at θ=63.5° while T^{L} tends to vanish. T^{U} can be increased due to the proper choice of the kL value. For example, in Fig. 9(c), $T^{\mathrm{U}}\approx 2t^{\mathrm{U}}_{-1}$, $t^{\mathrm{U}}_{-1}=t^{\mathrm{U}}_{-2}=0.297$, and T^{L}=0.044 at θ=64.15°.

3.4 Unidirectionality in purely metallic gratings

A unidirectional transmission can also be obtained by using purely metallic gratings. Figure 10 shows t_n vs kL for the two thin gratings with the same values of $\omega_p L/c$ and $\kappa_n L$, and θ as in Fig. 5(a). Correspondingly, the single-beam unidirectionality is realized due to the negative first order. Note that t_{-2} at $k>\kappa_2$ and t_{-3} at $k>\kappa_3$ show here rather small values. Furthermore, t_{-3} in Fig. 10(a) nearly vanishes. Therefore, the additional selectivity of the diffraction orders is expected to be realizable due to the optimization of the corrugation parameters and the use of a single metallic corrugated layer, instead of a two- or three-layer grating.

#111241 - $15.00 USD Received 11 May 2009; revised 9 Jul 2009; accepted 13 Jul 2009; published 20 Jul 2009

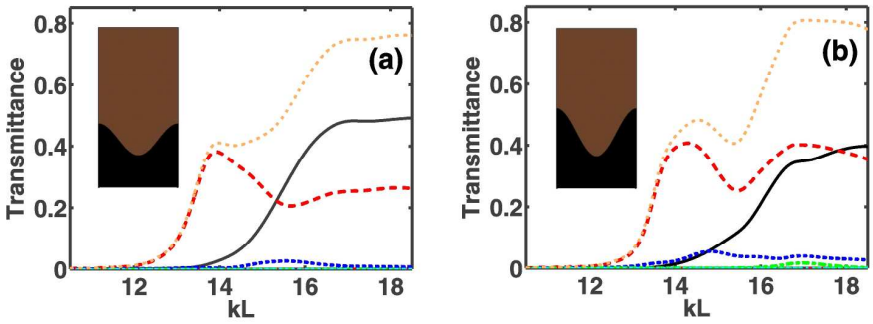

Fig. 10. Transmittance for purely metallic thin gratings in the U case at $\omega_p L/c=4\pi$, $\gamma/\omega_p=0.01$, and $\theta=\pi/6$; plot (a) - $A=0.3$, $B=0.1$, and $h/L=0.8$; plot (b) - $A=0.35$, $B=0.15$, and $h/L=1$; $C=D=0$ and $M=1$; black solid line - $n=0$, red dashed line - $n=-1$, blue thick dotted line - $n=-2$, green dashed-dotted line - $n=-3$, and orange thin dotted line – sum of all the propagating orders.

4. Conclusions

To summarize, we have studied diffraction on the gratings, which contain flat metallic and flat and corrugated dielectric layers. It was shown that the extrinsic wideband unidirectionality can be obtained in such non-symmetric intrinsically isotropic gratings, so that all the waves involved in the diffraction are linearly polarized. Significant transmission can occur if a grating is illuminated from the side of the corrugated interface but disappears if it is illuminated from the side of the non-corrugated interface. This effect is easily achieved by tilting, while the isofrequency dispersion contours are still isotropic for all the layers. The metallic layer plays the key role in the suggested mechanism, which is based on the fact that the zero order in air and dielectric can be uncoupled to the zero order in a collisionless metal, while at least one of the higher orders created in air by the upper-side corrugations is coupled to that in the metal. Since the corrugations only appear on one side of the grating, the transmission channel can be either open or closed, depending on whether the corrugated or non-corrugated interface is illuminated. Hence, the zero order is parasitic for achieving unidirectionality. However, in case of partial unidirectionality, the two-way (reciprocal) zero-order transmission co-exists with the one-way (non-reciprocal) higher-order transmission. Single-beam unidirectionality can be relatively strong within a frequency range that is adjacent to the plasma frequency. The largest transmission values were observed for the frequency values, which correspond to the multibeam unidirectionality. The presented examples show that more than 50 percent of the incident-wave energy can be transmitted in one direction only. Research on the possibility of obtaining reflection-free unidirectionality is currently in progress. Optimized unidirectional devices are expected to be obtainable for a proper selection of the geometrical and material parameters of the layers and the angle of incidence, providing one with an alternative to the use of anisotropic materials.

Acknowledgments

This work is supported by the European Union under the projects EU-PHOME and EU-ECONAM, and TUBITAK under the Project Nos. 106E198, 107A004, and 107A012. One of the authors (A.S.) also thanks TUBITAK for the partial support of this work in the framework of the Visiting Scientists Fellowship Program. One of the authors (E.O.) acknowledges partial support from the Turkish Academy of Sciences.

#111241 - $15.00 USD Received 11 May 2009; revised 9 Jul 2009; accepted 13 Jul 2009; published 20 Jul 2009